



Search for resonance-enhanced CP and angular asymmetries in the $\Lambda_c^+ \rightarrow p\mu^+\mu^-$ decay at LHCb

LHCb collaboration[†]

Abstract

The first measurement of the CP asymmetry of the decay rate (A_{CP}) and the CP average (ΣA_{FB}) and CP asymmetry (ΔA_{FB}) of the forward-backward asymmetry in the muon system of $\Lambda_c^+ \rightarrow p\mu^+\mu^-$ decays is reported. The measurement is performed using a data sample of proton-proton collisions, recorded by the LHCb experiment from 2016 to 2018 at a center-of-mass energy of 13 TeV, which corresponds to an integrated luminosity of 5.4 fb^{-1} . The asymmetries are measured in two regions of dimuon mass near the ϕ -meson mass peak. The dimuon-mass integrated results are

$$\begin{aligned} A_{CP} &= (-1.1 \pm 4.0 \pm 0.5)\%, \\ \Sigma A_{FB} &= (3.9 \pm 4.0 \pm 0.6)\%, \\ \Delta A_{FB} &= (3.1 \pm 4.0 \pm 0.4)\%, \end{aligned}$$

where the first uncertainty is statistical and the second systematic. The results are consistent with the conservation of CP symmetry and the Standard Model expectations.

Submitted to Phys. Rev. D

© 2025 CERN for the benefit of the LHCb collaboration. [CC BY 4.0 licence](#).

[†]Authors are listed at the end of this paper.

Rare decays that are sensitive to transitions between c and u quarks in association with the simultaneous emission of a pair of oppositely charged leptons ($\ell^+\ell^-$) offer the opportunity to explore flavor-changing neutral-currents (FCNCs) in the up-type quark sector. In the Standard Model (SM), FCNC transitions are only generated by loop-level processes and suppressed by the Glashow–Iliopoulos–Maiani (GIM) mechanism [1]. In the charm system, the GIM mechanism leads to a particularly strong suppression with respect to the down-type quark sector. Thus, studies of rare charm decays are sensitive probes of beyond-Standard-Model phenomena and constitute a complementary testing ground with respect to studies of rare beauty and strange hadron decays. New particles and interactions extending the SM can lead to modifications of branching fractions, modify angular distributions of final-state particles, or introduce additional sources of charge-parity (CP) asymmetry [2–15]. The LHCb collaboration has previously succeeded in measuring branching fractions of rare charm meson decays at the level of 10^{-7} and recently published the first angular analysis and a search for CP violation in rare decays of neutral D^0 mesons [16–19]. However, measurements of rare baryonic charm decays comprising two charged leptons in the final state remain far less explored in the experimental landscape [20–22].

The decays of Λ_c^+ baryons to $p\mu^+\mu^-$ final states¹ proceed at short distances via $c \rightarrow u\ell^+\ell^-$ transitions, which in the SM lead to branching fractions below $\mathcal{O}(10^{-8})$ [23–27]. However, the total decay width is dominated by intermediate resonant contributions of the form $\Lambda_c^+ \rightarrow pX(\rightarrow \mu^+\mu^-)$, where X can be a short-lived η , ρ^0 , ω or ϕ meson that subsequently decays into two muons. These long-distance contributions increase the branching fraction to $\mathcal{O}(10^{-6})$. Recently, the LHCb collaboration has published an updated measurement of the branching fractions of $\Lambda_c^+ \rightarrow p\mu^+\mu^-$ decays in different regions of the dimuon mass, $m(\mu^+\mu^-)$ [22]. The measurement is performed relative to the branching fraction in the $m(\mu^+\mu^-)$ region around the known ϕ -meson mass [28], which is the dominant contribution to the total decay rate. An upper limit on the branching fraction $\mathcal{B}(\Lambda_c^+ \rightarrow p\mu^+\mu^-) < 2.9 \times 10^{-8}$ at 90% confidence level is set in regions of $m(\mu^+\mu^-)$ where the influence of intermediate resonances is minimal and sensitivity to beyond-SM contributions is largest. Further separation of short and long-distance contributions can be reached by studying angular distributions and CP asymmetries, which complement searches for new phenomena in decays of D^0 and D^+ mesons because of the nonzero spin of the Λ_c^+ baryons [25–27]. However, to date, no measurements of CP or angular asymmetries in $\Lambda_c^+ \rightarrow p\mu^+\mu^-$ decays have been performed.

This letter presents the first measurement of the direct CP asymmetry, as well as the CP average and CP asymmetry of the forward-backward asymmetry in the lepton system, in $\Lambda_c^+ \rightarrow p\mu^+\mu^-$ decays. The analysis uses proton-proton (pp) collision data recorded by the LHCb experiment at a center-of-mass energy of 13 TeV in the years 2016, 2017 and 2018, which correspond to an integrated luminosity of 5.4 fb^{-1} . The analysis uses Λ_c^+ baryons produced directly in the primary pp interaction and the same data as used in Ref. [22]. However, the signal candidate selection is reoptimized for the measurement of asymmetries. The CP asymmetry, A_{CP} , is defined in terms of the difference of decay rates for Λ_c^+ and $\bar{\Lambda}_c^-$ decays to $p\mu^+\mu^-$ and $\bar{p}\mu^+\mu^-$ final states as

$$A_{CP} \equiv \frac{\Gamma(\Lambda_c^+ \rightarrow p\mu^+\mu^-) - \Gamma(\bar{\Lambda}_c^- \rightarrow \bar{p}\mu^+\mu^-)}{\Gamma(\Lambda_c^+ \rightarrow p\mu^+\mu^-) + \Gamma(\bar{\Lambda}_c^- \rightarrow \bar{p}\mu^+\mu^-)}, \quad (1)$$

¹Charge-conjugate decays are implied throughout this letter unless stated otherwise.

where Γ is the decay rate. The forward-backward asymmetry, A_{FB} , is defined as

$$A_{\text{FB}} \equiv \frac{\Gamma(\cos \theta > 0) - \Gamma(\cos \theta < 0)}{\Gamma(\cos \theta > 0) + \Gamma(\cos \theta < 0)}, \quad (2)$$

where θ is the angle between the direction of the positively charged lepton in the dimuon rest frame and the flight direction of the dimuon system in the rest frame of the Λ_c^+ baryon. In contrast, for $\bar{\Lambda}_c^-$ baryons the angle is measured relative to the flight direction of the negatively charged lepton. The forward-backward asymmetry is measured separately for Λ_c^+ and $\bar{\Lambda}_c^-$ baryons and referred to as $A_{\text{FB}}^{A_c^+}$ and $A_{\text{FB}}^{\bar{A}_c^-}$, respectively, which allows the CP average, $\Sigma A_{\text{FB}}^{CP}$, and the CP asymmetry, $\Delta A_{\text{FB}}^{CP}$, to be defined as

$$\begin{aligned} \Sigma A_{\text{FB}}^{CP} &\equiv 1/2 \cdot \left[A_{\text{FB}}^{A_c^+} + A_{\text{FB}}^{\bar{A}_c^-} \right], \\ \Delta A_{\text{FB}}^{CP} &\equiv 1/2 \cdot \left[A_{\text{FB}}^{A_c^+} - A_{\text{FB}}^{\bar{A}_c^-} \right]. \end{aligned} \quad (3)$$

These observables further enhance the sensitivity of the measurement to the real and imaginary parts of beyond-SM couplings [26].

Given the current experimental sensitivity, the asymmetries measured in this letter are null tests of the SM. Interference effects between SM resonant and beyond-SM amplitudes can produce asymmetries as large as $\mathcal{O}(\%)$ [25], referred to as *resonance enhanced* asymmetries. The measurement is performed in the $m(\mu^+\mu^-)$ region which is dominated by the intermediate ϕ meson, where the signal yield is sufficiently high to measure CP and angular asymmetries. To be sensitive to variations of the asymmetries over the phase space, the observables are determined in two regions, which are defined symmetrically below and above the known mass of the ϕ meson [28].

The LHCb detector [29, 30] is a single-arm forward spectrometer designed for the study of particles containing b or c quarks. It includes a high-precision tracking system consisting of a silicon-strip vertex detector surrounding the pp interaction region, a large-area silicon-strip detector located upstream of a dipole magnet with a bending power of about 4 Tm, and three stations of silicon-strip detectors and straw drift tubes placed downstream of the magnet. The polarity of the magnetic field is reversed periodically throughout the data-taking. Particle identification is provided by two ring-imaging Cherenkov detectors, an electromagnetic and a hadronic calorimeter, and a muon system composed of alternating layers of iron and multiwire proportional chambers. Events are selected online by a trigger that consists of a hardware stage, which is based on information from the calorimeter and muon systems, followed by a software stage which performs a full event reconstruction [31]. Simulation is required to model the effects of the detector acceptance, the imposed selection requirements and to describe the signal and backgrounds. In the simulation, pp collisions are generated using PYTHIA [32] with a specific LHCb configuration [33]. Decays of unstable particles are described by EVTGEN [34], in which final-state radiation is generated using PHOTOS [35]. The interaction of the generated particles with the detector, and its response, are implemented using the GEANT4 toolkit [36] as described in Ref. [37]. The underlying pp interaction is reused multiple times, with an independently generated signal decay for each [38].

The hardware trigger requires the presence of a muon with large transverse momentum, p_T , which is compatible with one of the two muons of the signal candidate. Furthermore, candidates where a positive trigger decision is caused by the presence of muons with high

p_T , or a hadron, photon or electron with high transverse energy in the calorimeters due to other particles produced in the pp collision, are also considered. The subsequent software trigger selects in a first stage events where a pair of tracks satisfies a multivariate classifier based on geometric and kinematic criteria that identifies candidates consistent with the displaced decay of a charm hadron, or alternatively events with a reconstructed dimuon vertex which is displaced from any primary vertex (PV). In the second software-trigger stage, candidate Λ_c^+ baryons are constructed by combining three charged tracks that form a good-quality secondary vertex. Each of the tracks is required to be inconsistent with originating from a PV, to satisfy $p_T > 0.3 \text{ GeV}/c$ and to have a minimum momentum p of $3 \text{ GeV}/c$. The scalar sum of the p_T of the three tracks has to exceed $0.5 \text{ GeV}/c$. The Λ_c^+ candidate must have a decay vertex significantly separated from any PV, and compatible with originating from one of the PVs. Therefore, only Λ_c^+ candidates with a reconstructed momentum vector that aligns with the vector connecting the secondary and primary vertices are further considered.

Additional selection criteria are applied offline. The reconstructed mass of the Λ_c^+ candidates, $m(p\mu^+\mu^-)$, is limited to the range $[2147, 2486] \text{ MeV}/c^2$. Stringent particle identification criteria are placed on the particles identified as protons to suppress background from misidentified $D^+ \rightarrow \pi^+\mu^+\mu^-$ decays, where the pion is wrongly identified as a proton. The selection is further optimized to reduce the contributions of two major sources of background. The first comprises random associations of unrelated tracks that coincidentally fulfill the selection criteria. To reduce this combinatorial background, a multivariate selection based on a boosted decision tree (BDT) classifier [39, 40] as implemented in the TMVA toolkit [41] is employed. The BDT classifier is trained using simulated candidates as proxies for the signal, and data candidates with $m(p\mu^+\mu^-) < 2256.5 \text{ MeV}/c^2$ or $m(p\mu^+\mu^-) > 2321.5 \text{ MeV}/c^2$ for the background. The AdaBoost algorithm [42] is used when training the BDT classifier in ten disjoint training subsamples, which is subsequently applied using a k -fold cross-validation [43]. The choice of features that are used in the training has been based on the selection described in Ref. [22] and comprises kinematic and topological features of the Λ_c^+ candidates, as well as features related to the isolation of the signal candidates with respect to other tracks in the event. The variables are chosen to minimize the correlation with the Λ_c^+ mass to avoid artificial sculpting of the mass spectrum of Λ_c^+ candidates.

The second major background arises from hadronic Λ_c^+ baryon decays to $p\pi^+\pi^-$ final states, where two oppositely charged pions are identified as muons. Despite the low pion to muon misidentification probability [44], the large branching fraction of $\Lambda_c^+ \rightarrow p\pi^+\pi^-$ decays [28] causes a peaking background. This is further suppressed by a multivariate muon-identification discriminant that combines the information from the Cherenkov detectors, the calorimeters and the muon chambers.

The threshold on the muon-identification discriminant is simultaneously optimized with the requirement on the BDT classifier output by minimizing the uncertainty on the asymmetries. This is achieved by randomly splitting the data samples into two halves, simulating a vanishing asymmetry in the samples as expected in null-test measurements.

If after the full selection an event contains more than one Λ_c^+ candidate, only one is randomly selected. This requirement removes less than one percent of candidates. To avoid potential biases on the measured quantities, all asymmetries were shifted by a random offset and only examined after the analysis procedure had been finalized.

The reconstruction and selection requirements result in efficiency losses that correlate

with the decay kinematics and vary as a function of $m(\mu^+\mu^-)$ and $\cos\theta$. A correction for relative efficiency variations across the phase space is applied using simulated samples to ensure an unbiased determination of the measured asymmetries. The simulation samples are corrected for known differences with respect to data in particle identification response [44]. A two-dimensional correction map is employed to assign weights to each candidate that account for relative efficiency variations and can be found in the supplemental material [45].

To determine A_{CP} , the so-called *raw* asymmetry, A_{raw} , is measured, which also receives contributions from nuisance asymmetries of approximately 4%. These asymmetries are caused by the different production cross-sections of Λ_c^+ and $\bar{\Lambda}_c^-$ baryons, quantified as the production asymmetry, $A_{\text{prod}}(\Lambda_c^+)$, and a nonequal detection efficiency of protons and antiprotons which leads to a detection asymmetry, $A_{\text{det}}(p)$. The detection asymmetry from the pair of oppositely charged muons is estimated to be negligible. For small asymmetries, the raw asymmetry can be approximated as

$$A_{\text{raw}}(\Lambda_c^+ \rightarrow p\mu^+\mu^-) \equiv \frac{N(\Lambda_c^+ \rightarrow p\mu^+\mu^-) - N(\bar{\Lambda}_c^- \rightarrow \bar{p}\mu^+\mu^-)}{N(\Lambda_c^+ \rightarrow p\mu^+\mu^-) + N(\bar{\Lambda}_c^- \rightarrow \bar{p}\mu^+\mu^-)} \quad (4)$$

$$\approx A_{CP}(\Lambda_c^+ \rightarrow p\mu^+\mu^-) + A_{\text{prod}}(\Lambda_c^+) + A_{\text{det}}(p)$$

The CP asymmetry is obtained by subtracting the raw asymmetry measured in a control data sample of $\Lambda_c^+ \rightarrow pK_S^0$ decays, where effects of CP violation are assumed to be negligible and which is subject to the same nuisance asymmetries, as

$$A_{CP}(\Lambda_c^+ \rightarrow p\mu^+\mu^-) = A_{\text{raw}}(\Lambda_c^+ \rightarrow p\mu^+\mu^-) - A_{\text{raw}}(\Lambda_c^+ \rightarrow pK_S^0). \quad (5)$$

Since $A_{\text{det}}(p)$ and $A_{\text{prod}}(\Lambda_c^+)$ depend on the kinematics of the p and Λ_c^+ particles, a weighting scheme is developed to match the final-state kinematics of the control mode to that of the signal mode using a BDT algorithm with gradient boosting [39–41].

To measure the asymmetries, the data are split in four disjoint subsamples, which are defined by the flavor of the Λ_c^+ baryon and the sign of $\cos\theta$. The measurement is performed separately in the two $m(\mu^+\mu^-)$ regions ϕ_{low} and ϕ_{high} , defined as [979.46, 1019.46] MeV/ c^2 and [1019.46, 1059.46] MeV/ c^2 . In the following, these dimuon-mass regions refer to ranges in the reconstructed dimuon mass, without correcting for effects due to a finite experimental mass resolution of approximately 8 MeV/ c^2 [45]. Figure 1 shows the background-subtracted dimuon-mass spectrum of $\Lambda_c^+ \rightarrow p\mu^+\mu^-$ candidates using a sideband subtraction, with the boundary between the two $m(\mu^+\mu^-)$ ranges also indicated.

The asymmetries are then determined through unbinned extended maximum-likelihood fits to the weighted $m(p\mu^+\mu^-)$ distribution of selected candidates, where the weights correct for the phase-space-dependent efficiency variations. The asymmetries and yields are determined from simultaneous fits, in which they are treated as free parameters. The total fit function consists of three components: the $\Lambda_c^+ \rightarrow p\mu^+\mu^-$ signal, combinatorial background and background from misidentified $\Lambda_c^+ \rightarrow p\pi^+\pi^-$ decays. The signal component is described by the sum of a Johnson S_U function [46] and a Gaussian function, to account for asymmetric tails of the distribution. The parameters of the model are determined by a fit to simulated candidates which are selected with the same requirements as the data candidates. The peak position of the distribution is allowed to vary in the fit to the data separately for the two dimuon-mass regions and baryon flavors. The mass shape of the combinatorial background is parameterized using a fourth-order Chebyshev

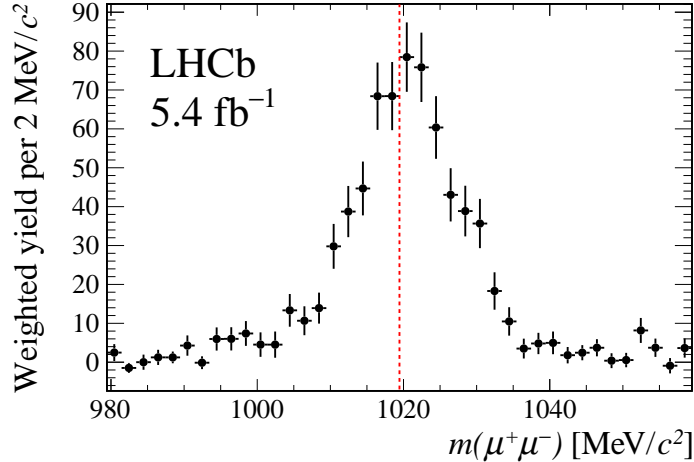


Figure 1: Background-subtracted distribution of dimuon mass for $\Lambda_c^+ \rightarrow p\mu^+\mu^-$ candidates. The red line indicates the known mass of the ϕ meson, which marks the boundary between the two considered dimuon-mass regions. Weights are assigned to correct for efficiency variations as described in the main text.

Table 1: Yields after correcting for relative efficiency variations and measured asymmetries for $\Lambda_c^+ \rightarrow p\mu^+\mu^-$ decays in the two dimuon-mass regions. For the asymmetries the first uncertainty is statistical and the second systematic.

$m(\mu^+\mu^-)$	Efficiency-weighted yields			Asymmetries		
	Signal	Misid. back.	Comb. back.	A_{CP} [%]	$A_{FB}^{A_c^+}$ [%]	$A_{FB}^{\bar{A}_c^-}$ [%]
ϕ_{low}	346 ± 22	57 ± 21	437 ± 26	$-0.8 \pm 6.2 \pm 0.6$	$11.7 \pm 8.5 \pm 1.1$	$2.2 \pm 8.7 \pm 1.4$
ϕ_{high}	435 ± 22	35 ± 17	390 ± 25	$-1.4 \pm 5.3 \pm 0.6$	$3.5 \pm 7.2 \pm 0.9$	$-0.3 \pm 7.4 \pm 1.1$

polynomial with parameters determined by a fit to a control data sample, where all three final-state particles carry the same electric charge. These candidates are entirely made of random combinations of tracks and used as a proxy for the combinatorial background. The misidentified $\Lambda_c^+ \rightarrow p\pi^+\pi^-$ background is also described by a Johnson S_U function [46] whose parameters are determined using simulated candidates of $\Lambda_c^+ \rightarrow p\pi^+\pi^-$ decays assigning the muon mass hypothesis to both pions. Due to limited simulation sample sizes, not all selection criteria can be applied and the requirement on muon particle identification is applied to only one of the two pions. The CP and forward-backward asymmetries of misidentified background are determined using high-yield data control samples of $\Lambda_c^+ \rightarrow p\pi^+\pi^-$ decays and are fixed in the baseline fit that is used to measure the asymmetries. Assumptions in the background modeling give rise to systematic uncertainties which are described later in this letter.

In the fit, the free parameters are the yields of each fit component, the asymmetries of signal and combinatorial background, and the signal peak position. The fits are performed separately in the two dimuon-mass regions. The fits are validated to return unbiased estimates of the asymmetries and their uncertainties using large samples of pseudoexperiments. The resulting signal and background yields, as well as the asymmetries A_{CP} , $A_{FB}^{A_c^+}$ and $A_{FB}^{\bar{A}_c^-}$ are listed in Table 1. The mass spectrum of selected $\Lambda_c^+ \rightarrow p\mu^+\mu^-$ candidates is shown in Fig. 2, together with the fit projection.

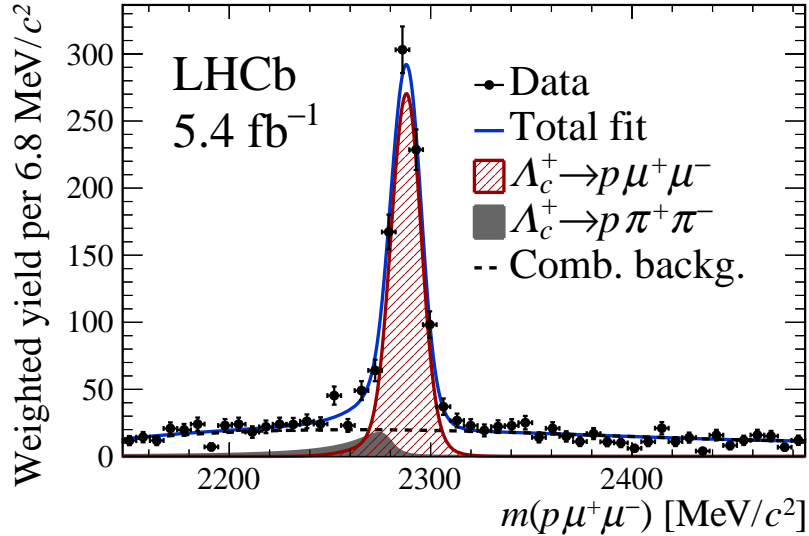


Figure 2: Distribution of $m(p\mu^+\mu^-)$ for efficiency-weighted candidates, together with the fit projection.

The dominant systematic uncertainties affect all asymmetries and arise from limited knowledge of the models used in the mass fits and possible imperfections in the correction for phase-space-dependent efficiency variations. To evaluate the systematic uncertainty related to the fit model, pseudoexperiments are performed, where alternative parametrizations of the signal and background components are tested against the baseline fit model. For the signal component, a Crystal Ball function [47] and a Gaussian function are chosen as alternatives. In addition, the requirements used to select the control sample to determine the shape of the combinatorial background are varied, and an alternative shape is obtained from a fit, where the shape parameters are left free to vary when fitting $\Lambda_c^+ \rightarrow p\mu^+\mu^-$ signal candidates. To address the inability to apply the signal muon particle-identification requirements on the simulated $\Lambda_c^+ \rightarrow p\pi^+\pi^-$ decays, an alternative shape is determined on a sample where muon particle identification requirements are not applied. The asymmetries of the misidentified background component, which are fixed in the baseline fit, are determined in control samples with modified selection requirements and varied within the observed deviations from the baseline values. The studies are performed separately for both dimuon-mass regions. For all tested alternatives, the mean bias with respect to the baseline model is determined for the measured asymmetries, and the largest observed bias over the set of shape variations in each dimuon-mass region is taken as the corresponding systematic uncertainty.

Systematic uncertainties related to the correction for efficiency variations are evaluated by creating alternative correction maps targeting aspects of the selection which might be subject to residual differences in simulation and data. The alternative maps are obtained by applying weights to the simulated candidates to match the number of reconstructed tracks and the BDT output distribution observed in data, and by placing requirements on particle identification for the final-state particles neglecting the corrections that are applied in the baseline analysis. Using the alternative correction maps, the measurement is repeated on resampled data sets which are obtained by bootstrapping the original sample [48]. The root mean square among the variations of the results that are observed

Table 2: CP average and asymmetry of the forward-backward asymmetry for $\Lambda_c^+ \rightarrow p\mu^+\mu^-$ decays in the dimuon-mass regions. The first uncertainty is statistical and the second systematic.

$m(\mu^+\mu^-)$	$\Sigma A_{\text{FB}} [\%]$	$\Delta A_{\text{FB}} [\%]$
ϕ_{low}	$6.9 \pm 6.1 \pm 1.0$	$4.8 \pm 6.1 \pm 0.8$
ϕ_{high}	$1.6 \pm 5.2 \pm 0.8$	$1.9 \pm 5.2 \pm 0.6$

with the alternative maps is taken as the systematic uncertainty. The uncertainty related to the limited simulation sample size is also propagated and considered as systematic uncertainty on the measured asymmetries.

Additionally, the following three sources of systematic uncertainty are only relevant for the measurement of A_{CP} . The first source arises from the instrumental asymmetry correction due to limitations of the kinematic equalization procedure. A systematic uncertainty is assigned by evaluating the effect of residual discrepancies of the kinematic distributions of signal and control mode candidates after the weighting. The root mean square among the variations of the results obtained after a second one-dimensional weighting of the Λ_c^+ and proton kinematic distributions is taken as a systematic uncertainty. The second source arises from the combined effects of CP violation and mixing in the neutral kaon system and the different interaction probabilities of K^0 and \bar{K}^0 particles with the detector material [49, 50] and a systematic uncertainty is evaluated following the method described in Refs. [51, 52]. Finally, the fraction of Λ_c^+ baryons arising from decays of b -flavored hadrons is determined for signal and control mode candidates by studying the distribution of the impact parameter, which is defined as the minimum distance of the Λ_c^+ trajectory to the PV. The difference of these fractions for signal and control mode candidates, together with the difference in asymmetries for Λ_c^+ baryons produced in the primary interaction and from b -hadron decays, are translated into a systematic uncertainty related to an imperfect cancellation of production asymmetries.

The finite angular resolution of the LHCb detector is relevant for the measurement of the forward-backward asymmetry, and a systematic uncertainty is assigned by estimating the fraction of candidates where the sign of $\cos\theta$ changes due to the finite detector resolution in simulations.

A summary of the systematic uncertainties, together with the correlations of the measured asymmetries due to the systematic uncertainties, can be found in the supplemental material of this letter [45]. The size of the systematic uncertainty depends on the considered asymmetry and dimuon-mass region but typically constitutes between 10% and 15% of the corresponding statistical uncertainty.

The analysis is repeated on statistically independent data subsets to check for biases from specific instrumental effects. The criteria to split the subsets include the number of PVs and reconstructed tracks in the event, the data-taking year, the magnetic-field orientation, the trigger classification, the Λ_c^+ baryon transverse momentum and the impact parameter significance of the Λ_c^+ candidate with respect to the PV, which is defined as the difference in the vertex-fit χ^2 of a given PV, reconstructed with and without considering the candidate. The resulting variations of the measured asymmetries are consistent with statistical fluctuations.

Using Eq. 3 and considering correlations between the systematic uncertainties [45],

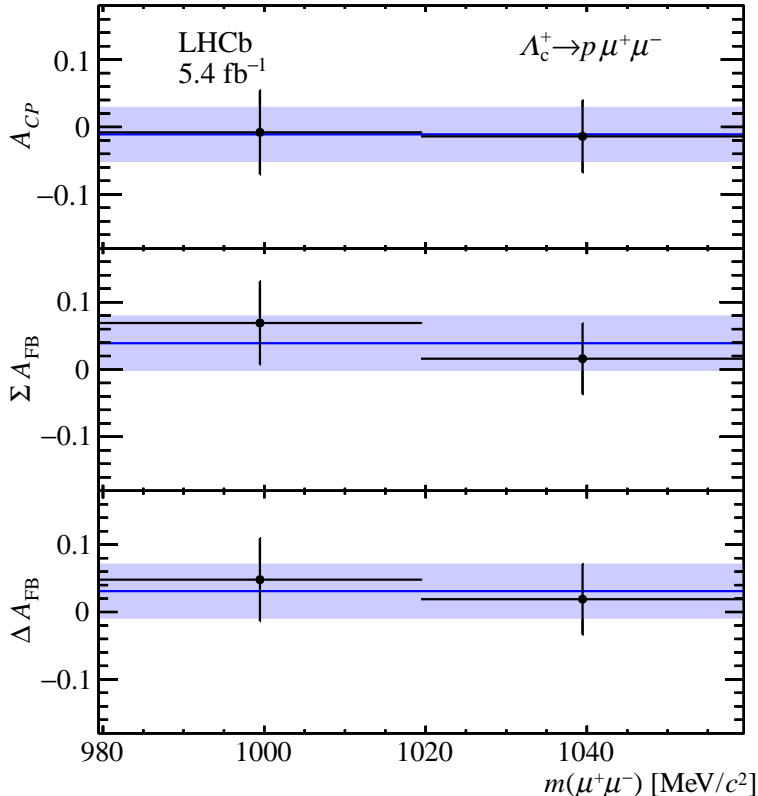


Figure 3: Measured signal asymmetries in the regions of dimuon mass (black points) and their dimuon-mass-integrated value with its uncertainty (blue). The shown uncertainty comprises both the statistical and systematic uncertainty.

ΔA_{FB} and ΣA_{FB} are computed from the measured asymmetries listed in Table 1 and the results can be found in Table 2. Correlations between the statistical uncertainties of the measured asymmetries are negligible. Furthermore, the dimuon-mass integrated values are determined, following the procedure described in Ref. [53], and found to be:

$$\begin{aligned}
 A_{CP} &= (-1.1 \pm 4.0 \pm 0.5)\%, \\
 \Sigma A_{\text{FB}} &= (3.9 \pm 4.0 \pm 0.6)\%, \\
 \Delta A_{\text{FB}} &= (3.1 \pm 4.0 \pm 0.4)\%,
 \end{aligned}$$

where the first uncertainty is statistical and the second systematic. All results are also shown in Fig. 3 and are consistent with zero, confirming the SM expectation.

In summary, a search for resonance-enhanced angular and CP asymmetries in $\Lambda_c^+ \rightarrow p\mu^+\mu^-$ decays in two $m(\mu^+\mu^-)$ regions near the ϕ -meson mass is presented. The results are based on the analysis of pp collision data recorded by the LHCb experiment in the years 2016, 2017 and 2018 at a center-of-mass energy of 13 TeV, which correspond to an integrated luminosity of 5.4 fb^{-1} . The asymmetries are measured in two regions of dimuon mass to enhance the sensitivity to beyond-SM effects. The results confirm the SM prediction and will help to constrain the parameter space of models extending the SM [25, 26]. Future data sets recorded by the upgraded LHCb detector [54] with significantly increased yields will allow the statistical uncertainties to be further reduced, and the measurement to be extended to additional dimuon-mass regions.

Acknowledgements

We express our gratitude to our colleagues in the CERN accelerator departments for the excellent performance of the LHC. We thank the technical and administrative staff at the LHCb institutes. We acknowledge support from CERN and from the national agencies: CAPES, CNPq, FAPERJ and FINEP (Brazil); MOST and NSFC (China); CNRS/IN2P3 (France); BMBF, DFG and MPG (Germany); INFN (Italy); NWO (Netherlands); MNiSW and NCN (Poland); MCID/IFA (Romania); MICIU and AEI (Spain); SNSF and SER (Switzerland); NASU (Ukraine); STFC (United Kingdom); DOE NP and NSF (USA). We acknowledge the computing resources that are provided by CERN, IN2P3 (France), KIT and DESY (Germany), INFN (Italy), SURF (Netherlands), PIC (Spain), GridPP (United Kingdom), CSCS (Switzerland), IFIN-HH (Romania), CBPF (Brazil), and Polish WLCG (Poland). We are indebted to the communities behind the multiple open-source software packages on which we depend. Individual groups or members have received support from ARC and ARDC (Australia); Key Research Program of Frontier Sciences of CAS, CAS PIFI, CAS CCEPP, Fundamental Research Funds for the Central Universities, and Sci. & Tech. Program of Guangzhou (China); Minciencias (Colombia); EPLANET, Marie Skłodowska-Curie Actions, ERC and NextGenerationEU (European Union); A*MIDEX, ANR, IPhU and Labex P2IO, and Région Auvergne-Rhône-Alpes (France); AvH Foundation (Germany); ICSC (Italy); Severo Ochoa and María de Maeztu Units of Excellence, GVA, XuntaGal, GENCAT, InTalent-Inditex and Prog. Atracción Talento CM (Spain); SRC (Sweden); the Leverhulme Trust, the Royal Society and UKRI (United Kingdom).

References

- [1] S. L. Glashow, J. Iliopoulos, and L. Maiani, *Weak interactions with lepton-hadron symmetry*, *Phys. Rev.* **D2** (1970) 1285.
- [2] S. Fajfer and S. Prelovšek, *Effects of littlest Higgs model in rare D meson decays*, *Phys. Rev.* **D73** (2006) 054026, [arXiv:hep-ph/0511048](#).
- [3] I. I. Bigi and A. Paul, *On CP asymmetries in two-, three- and four-body D decays*, *JHEP* **03** (2012) 021, [arXiv:1110.2862](#).
- [4] S. Fajfer and N. Košnik, *Resonance catalyzed CP asymmetries in $D \rightarrow P\ell^+\ell^-$* , *Phys. Rev.* **D87** (2013) 054026, [arXiv:1208.0759](#).
- [5] L. Cappiello, O. Catà, and G. D'Ambrosio, *Standard model prediction and new physics tests for $D^0 \rightarrow h_1^+ h_2^- \ell^+ \ell^-$ ($h = \pi, K; \ell = e, \mu$)*, *JHEP* **04** (2013) 135, [arXiv:1209.4235](#).
- [6] A. Paul, A. de la Puente, and I. I. Bigi, *Manifestations of warped extra dimension in rare charm decays and asymmetries*, *Phys. Rev.* **D90** (2014) 014035, [arXiv:1212.4849](#).
- [7] S. Fajfer and N. Košnik, *Prospects of discovering new physics in rare charm decays*, *Eur. Phys. J.* **C75** (2015) 567, [arXiv:1510.00965](#).

- [8] S. de Boer and G. Hiller, *Flavour and new physics opportunities with rare charm decays into leptons*, *Phys. Rev.* **D93** (2016) 074001, [arXiv:1510.00311](#).
- [9] S. De Boer and G. Hiller, *Null tests from angular distributions in $D \rightarrow P_1 P_2 l^+ l^-$, $l = e, \mu$ decays on and off peak*, *Phys. Rev.* **D98** (2018) 035041, [arXiv:1805.08516](#).
- [10] R. Bause, M. Golz, G. Hiller, and A. Tayduganov, *The new physics reach of null tests with $D \rightarrow \pi \ell \ell$ and $D_s \rightarrow K \ell \ell$ decays*, *Eur. Phys. J.* **C80** (2020) 65, Erratum *ibid.* **C81** (2021) 219, [arXiv:1909.11108](#).
- [11] R. Bause, H. Gisbert, M. Golz, and G. Hiller, *Exploiting CP-asymmetries in rare charm decays*, *Phys. Rev.* **D101** (2020) 115006, [arXiv:2004.01206](#).
- [12] H. Gisbert, M. Golz, and D. S. Mitzel, *Theoretical and experimental status of rare charm decays*, *Mod. Phys. Lett.* **A36** (2021) 2130002, [arXiv:2011.09478](#).
- [13] A. Bharucha, D. Boito, and C. Méaux, *Disentangling QCD and new physics in $D^+ \rightarrow \pi^+ \ell^+ \ell^-$* , *JHEP* **04** (2021) 158, [arXiv:2011.12856](#).
- [14] S. Fajfer, E. Solomonidi, and L. Vale Silva, *S-wave contribution to rare $D^0 \rightarrow \pi^+ \pi^- \ell^+ \ell^-$ decays in the standard model and sensitivity to new physics*, *Phys. Rev.* **D109** (2024) 3, [arXiv:2312.07501](#).
- [15] M. Mandal, S. Biswas, S. Mahata, and S. Sahoo, *Searching for new physics in $c \rightarrow \mu$ transitions with nonuniversal Z' model*, *Int. J. Mod. Phys.* **A39** (2024) 2450063.
- [16] LHCb collaboration, R. Aaij *et al.*, *Observation of D^0 meson decays to $\pi^+ \pi^- \mu^+ \mu^-$ and $K^+ K^- \mu^+ \mu^-$ final states*, *Phys. Rev. Lett.* **119** (2017) 181805, [arXiv:1707.08377](#).
- [17] LHCb collaboration, R. Aaij *et al.*, *Measurement of angular and CP asymmetries in $D^0 \rightarrow \pi^+ \pi^- \mu^+ \mu^-$ and $D^0 \rightarrow K^+ K^- \mu^+ \mu^-$ decays*, *Phys. Rev. Lett.* **121** (2018) 091801, [arXiv:1806.10793](#).
- [18] LHCb collaboration, R. Aaij *et al.*, *Angular analysis of $D^0 \rightarrow \pi^+ \pi^- \mu^+ \mu^-$ and $D^0 \rightarrow K^+ K^- \mu^+ \mu^-$ decays and search for CP violation*, *Phys. Rev. Lett.* **128** (2022) 221801, [arXiv:2111.03327](#).
- [19] LHCb collaboration, R. Aaij *et al.*, *Search for D^0 meson decays to $\pi^+ \pi^- e^+ e^-$ and $K^+ K^- e^+ e^-$ final states*, [arXiv:2412.09414](#), Submitted to *Phys. Rev. Lett.*
- [20] K. Kodama *et al.*, *Upper limits for charm hadron decays to two muons plus hadrons*, *Phys. Lett.* **B345** (1995) 85.
- [21] BaBar collaboration, J. P. Lees *et al.*, *Searches for rare or forbidden semileptonic charm decays*, *Phys. Rev.* **D84** (2011) 072006, [arXiv:1107.4465](#).
- [22] LHCb collaboration, R. Aaij *et al.*, *Search for the rare decay of charmed baryon Λ_c^+ into the $p \mu^+ \mu^-$ final state*, *Phys. Rev.* **D110** (2024) 052007, [arXiv:2407.11474](#).
- [23] S. Meinel, *$\Lambda_c \rightarrow N$ form factors from lattice QCD and phenomenology of $\Lambda_c \rightarrow n \ell^+ \nu_\ell$ and $\Lambda_c \rightarrow p \mu^+ \mu^-$ decays*, *Phys. Rev.* **D97** (2018) 034511, [arXiv:1712.05783](#).

- [24] R. N. Faustov and V. O. Galkin, *Rare $\Lambda_c \rightarrow p\ell^+\ell^-$ decay in the relativistic quark model*, *Eur. Phys. J.* **C78** (2018) 527, [arXiv:1805.02516](#).
- [25] M. Golz, G. Hiller, and T. Magorsch, *Probing for new physics with rare charm baryon (Λ_c , Ξ_c , Ω_c) decays*, *JHEP* **09** (2021) 208, [arXiv:2107.13010](#).
- [26] H. Gisbert, G. Hiller, and D. Suelmann, *Effective field theory analysis of rare $|\Delta c| = |\Delta u| = 1$ charm decays*, *JHEP* **12** (2024) 102, [arXiv:2410.00115](#).
- [27] S.-Q. Zhang and C.-F. Qiao, *Rare Λ_c decays and new physics effects*, *Phys. Rev.* **D110** (2024) 114040, [arXiv:2411.15857](#).
- [28] Particle Data Group, S. Navas *et al.*, *Review of particle physics*, *Phys. Rev.* **D110** (2024) 030001.
- [29] LHCb collaboration, A. A. Alves Jr. *et al.*, *The LHCb detector at the LHC*, *JINST* **3** (2008) S08005.
- [30] LHCb collaboration, R. Aaij *et al.*, *LHCb detector performance*, *Int. J. Mod. Phys.* **A30** (2015) 1530022, [arXiv:1412.6352](#).
- [31] LHCb collaboration, R. Aaij *et al.*, *Measurement of the mass difference between neutral charm-meson eigenstates*, *Phys. Rev. Lett.* **122** (2019) 231802, [arXiv:1903.03074](#).
- [32] T. Sjöstrand, S. Mrenna, and P. Skands, *A brief introduction to PYTHIA 8.1*, *Comput. Phys. Commun.* **178** (2008) 852, [arXiv:0710.3820](#); T. Sjöstrand, S. Mrenna, and P. Skands, *PYTHIA 6.4 physics and manual*, *JHEP* **05** (2006) 026, [arXiv:hep-ph/0603175](#).
- [33] I. Belyaev *et al.*, *Handling of the generation of primary events in Gauss, the LHCb simulation framework*, *J. Phys. Conf. Ser.* **331** (2011) 032047.
- [34] D. J. Lange, *The EvtGen particle decay simulation package*, *Nucl. Instrum. Meth.* **A462** (2001) 152.
- [35] N. Davidson, T. Przedzinski, and Z. Was, *PHOTOS interface in C++: Technical and physics documentation*, *Comp. Phys. Comm.* **199** (2016) 86, [arXiv:1011.0937](#).
- [36] Geant4 collaboration, J. Allison *et al.*, *Geant4 developments and applications*, *IEEE Trans. Nucl. Sci.* **53** (2006) 270; Geant4 collaboration, S. Agostinelli *et al.*, *Geant4: A simulation toolkit*, *Nucl. Instrum. Meth.* **A506** (2003) 250.
- [37] M. Clemencic *et al.*, *The LHCb simulation application, Gauss: Design, evolution and experience*, *J. Phys. Conf. Ser.* **331** (2011) 032023.
- [38] D. Müller, M. Clemencic, G. Corti, and M. Gersabeck, *ReDecay: A novel approach to speed up the simulation at LHCb*, *Eur. Phys. J.* **C78** (2018) 1009, [arXiv:1810.10362](#).
- [39] L. Breiman, J. H. Friedman, R. A. Olshen, and C. J. Stone, *Classification and regression trees*, Wadsworth international group, Belmont, California, USA, 1984.

- [40] B. P. Roe *et al.*, *Boosted decision trees as an alternative to artificial neural networks for particle identification*, *Nucl. Instrum. Meth.* **A543** (2005) 577, [arXiv:physics/0408124](#).
- [41] A. Hoecker *et al.*, *TMVA - Toolkit for Multivariate Data Analysis*, PoS **ACAT** (2007) 040, [arXiv:physics/0703039](#).
- [42] Y. Freund and R. E. Schapire, *A decision-theoretic generalization of on-line learning and an application to boosting*, *J. Comput. Syst. Sci.* **55** (1997) 119.
- [43] A. Blum, A. Kalai, and J. Langford, *Beating the hold-out: bounds for k-fold and progressive cross-validation*, COLT '99 Proceedings of the twelfth annual conference on Computational learning theory (1999) 203.
- [44] R. Aaij *et al.*, *Selection and processing of calibration samples to measure the particle identification performance of the LHCb experiment in Run 2*, *Eur. Phys. J. Tech. Instr.* **6** (2019) 1, [arXiv:1803.00824](#).
- [45] See supplemental material for the efficiency map of $\Lambda_c^+ \rightarrow p\mu^+\mu^-$ decays, the dimuon-mass resolution, as well as a table of the systematic uncertainties and the correlation matrix for the measured asymmetries.
- [46] N. L. Johnson, *Systems of frequency curves generated by methods of translation*, *Biometrika* **36** (1949) 149.
- [47] T. Skwarnicki, *A study of the radiative cascade transitions between the Upsilon-prime and Upsilon resonances*, PhD thesis, Institute of Nuclear Physics, Krakow, 1986, DESY-F31-86-02.
- [48] B. Efron, *Bootstrap methods: Another look at the jackknife*, *Ann. Statist.* **7** (1979) 1.
- [49] A. Gsponer *et al.*, *Precise coherent K_S regeneration amplitudes for c , al , cu , sn , and pb nuclei from 20 to 140 gev/c and their interpretation*, *Phys. Rev. Lett.* **42** (1979) 13.
- [50] R. A. Briere and B. Winstein, *Determining the phase of a strong scattering amplitude from its momentum dependence to better than 1° : The example of kaon regeneration*, *Phys. Rev. Lett.* **75** (1995) 402.
- [51] LHCb collaboration, R. Aaij *et al.*, *Measurement of CP asymmetry in $D^0 \rightarrow K^-K^+$ and $D^0 \rightarrow \pi^-\pi^+$ decays*, *JHEP* **07** (2014) 041, [arXiv:1405.2797](#).
- [52] LHCb collaboration, R. Aaij *et al.*, *Measurement of the time-integrated CP asymmetry in $D^0 \rightarrow K^-K^+$ decays*, *Phys. Rev. Lett.* **131** (2023) 091802, [arXiv:2209.03179](#).
- [53] L. Lyons, D. Gibaut, and P. Clifford, *How to combine correlated estimates of a single physical quantity*, *Nucl. Instrum. Meth.* **A270** (1988) 110.
- [54] LHCb collaboration, R. Aaij *et al.*, *The LHCb Upgrade I*, *JINST* **19** (2024) P05065, [arXiv:2305.10515](#).

Supplemental material for the Letter “Search for resonance-enhanced CP and angular asymmetries in the $\Lambda_c^+ \rightarrow p\mu^+\mu^-$ decay at LHCb”

The two-dimensional efficiency map used to correct for the relative phase-space-dependent efficiency variations is shown in Fig. S1. Figure S2 shows the dimuon-mass resolution as obtained from simulated samples. The summary of the systematic uncertainties on the measured signal asymmetries can be found in Table S1. The correlation matrix for the systematic uncertainties between the measured signal asymmetries can be found in Table S2. The measurements are assumed to be statistically independent.

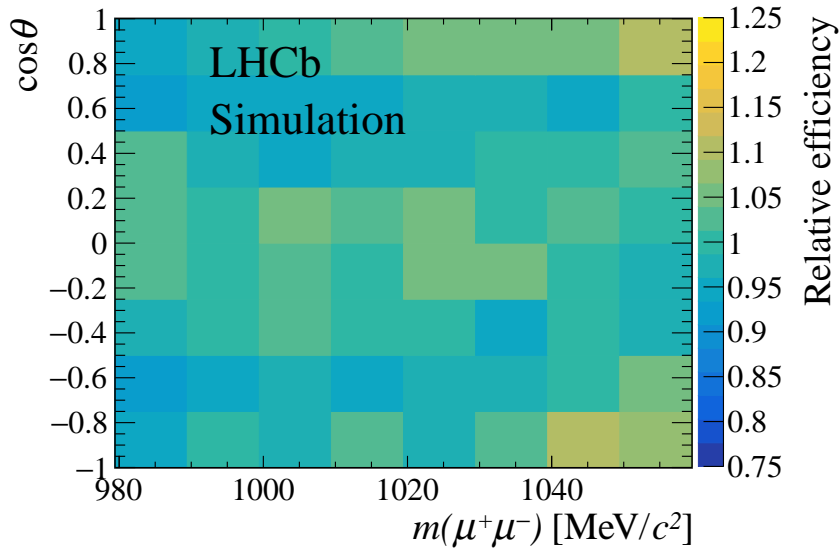


Figure S1: Two-dimensional efficiency map to correct for relative phase-space-dependent efficiency variations of selected $\Lambda_c^+ \rightarrow p\mu^+\mu^-$ candidates.

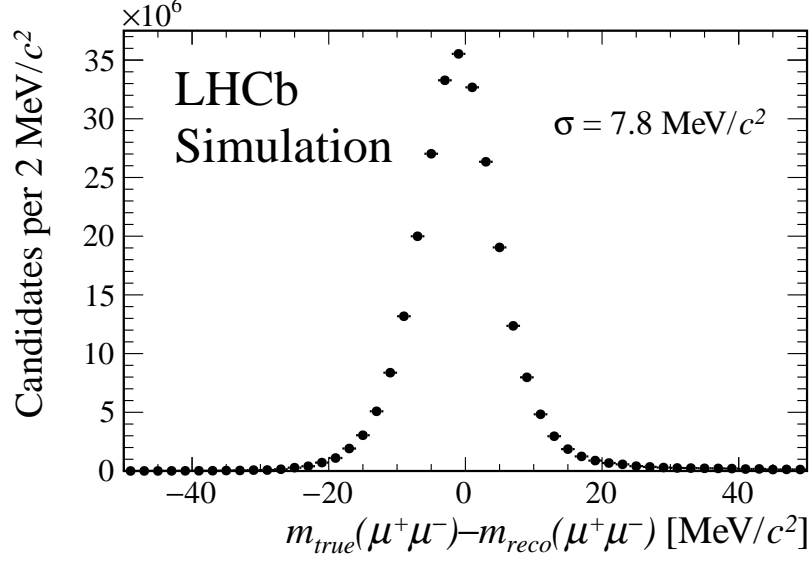


Figure S2: Dimuon-mass resolution of simulated $\Lambda_c^+ \rightarrow p\mu^+\mu^-$ candidates.

Table S1: Summary of the individual contributions to the systematic uncertainties on the observables, as well as the total systematic uncertainties. Dashes indicate sources which are inapplicable for the respective observable.

	Systematic uncertainty σ_A [10^{-2}]					
	$A_{CP\phi_{low}}$	$A_{FB}^{\Lambda_c^+}\phi_{low}$	$A_{FB}^{\bar{\Lambda}_c^-}\phi_{low}$	$A_{CP\phi_{high}}$	$A_{FB}^{\Lambda_c^+}\phi_{high}$	$A_{FB}^{\bar{\Lambda}_c^-}\phi_{high}$
Mass model	0.4	0.5	0.8	0.3	0.5	0.8
Efficiency correction	0.2	0.8	0.9	0.3	0.4	0.5
Simulation sample size	0.1	0.6	0.7	0.1	0.6	0.6
Kinematic weighting	0.2	—	—	0.2	—	—
Neutral kaon asymmetry	< 0.1	—	—	< 0.1	—	—
Λ_c^+ baryons from b hadrons	0.3	—	—	0.3	—	—
Angular resolution	—	< 0.1	< 0.1	—	< 0.1	< 0.1
Total systematic uncertainty	0.6	1.1	1.4	0.6	0.9	1.1

Table S2: Correlation matrix for the total systematic uncertainties.

	$A_{CP\phi_{low}}$	$A_{CP\phi_{high}}$	$A_{FB}^{\Lambda_c^+}\phi_{low}$	$A_{FB}^{\bar{\Lambda}_c^-}\phi_{low}$	$A_{FB}^{\Lambda_c^+}\phi_{high}$	$A_{FB}^{\bar{\Lambda}_c^-}\phi_{high}$
$A_{CP\phi_{low}}$	1	0.43	0	0	0	0
$A_{CP\phi_{high}}$		1	0	0	0	0
$A_{FB}^{\Lambda_c^+}\phi_{low}$			1	0.28	0	0
$A_{FB}^{\bar{\Lambda}_c^-}\phi_{low}$				1	0	0
$A_{FB}^{\Lambda_c^+}\phi_{high}$					1	0.34
$A_{FB}^{\bar{\Lambda}_c^-}\phi_{high}$						1

LHCb collaboration

R. Aaij³⁸ , A.S.W. Abdelmotteleb⁵⁷ , C. Abellan Beteta⁵¹ , F. Abudinén⁵⁷ ,
T. Ackernley⁶¹ , A. A. Adefisoye⁶⁹ , B. Adeva⁴⁷ , M. Adinolfi⁵⁵ , P. Adlarson⁸³ ,
C. Agapopoulou¹⁴ , C.A. Aidala⁸⁵ , Z. Ajaltouni¹¹ , S. Akar¹¹ , K. Akiba³⁸ ,
P. Albicocco²⁸ , J. Albrecht^{19,f} , F. Alessio⁴⁹ , M. Alexander⁶⁰ , Z. Aliouche⁶³ ,
P. Alvarez Cartelle⁵⁶ , R. Amalric¹⁶ , S. Amato³ , J.L. Amey⁵⁵ , Y. Amhis¹⁴ ,
L. An⁶ , L. Anderlini²⁷ , M. Andersson⁵¹ , A. Andreianov⁴⁴ , P. Andreola⁵¹ ,
M. Andreotti²⁶ , D. Andreou⁶⁹ , A. Anelli^{31,o,49} , D. Ao⁷ , F. Archilli^{37,u} ,
M. Argenton²⁶ , S. Arguedas Cuendis^{9,49} , A. Artamonov⁴⁴ , M. Artuso⁶⁹ ,
E. Aslanides¹³ , R. Ataíde Da Silva⁵⁰ , M. Atzeni⁶⁵ , B. Audurier¹² , D. Bacher⁶⁴ ,
I. Bachiller Perea¹⁰ , S. Bachmann²² , M. Bachmayer⁵⁰ , J.J. Back⁵⁷ ,
P. Baladron Rodriguez⁴⁷ , V. Balagura¹⁵ , A. Balboni²⁶ , W. Baldini²⁶ , L. Balzani¹⁹ ,
H. Bao⁷ , J. Baptista de Souza Leite⁶¹ , C. Barbero Pretel^{47,12} , M. Barbetti²⁷ , I.
R. Barbosa⁷⁰ , R.J. Barlow⁶³ , M. Barnyakov²⁵ , S. Barsuk¹⁴ , W. Barter⁵⁹ ,
J. Bartz⁶⁹ , J.M. Basels¹⁷ , S. Bashir⁴⁰ , G. Bassi^{35,r} , B. Batsukh⁵ , P. B.
Battista¹⁴ , A. Bay⁵⁰ , A. Beck⁶⁵ , M. Becker¹⁹ , F. Bedeschi³⁵ , I.B. Bediaga² , N. A.
Behling¹⁹ , S. Belin⁴⁷ , K. Belous⁴⁴ , I. Belov²⁹ , I. Belyaev³⁶ , G. Benane¹³ ,
G. Bencivenni²⁸ , E. Ben-Haim¹⁶ , A. Berezhnoy⁴⁴ , R. Bernet⁵¹ , S. Bernet Andres⁴⁵ ,
A. Bertolin³³ , C. Betancourt⁵¹ , F. Betti⁵⁹ , J. Bex⁵⁶ , Ia. Bezshyiko⁵¹ , J. Bhom⁴¹ ,
M.S. Bieker¹⁹ , N.V. Biesuz²⁶ , P. Billoir¹⁶ , A. Biolchini³⁸ , M. Birch⁶² ,
F.C.R. Bishop¹⁰ , A. Bitadze⁶³ , A. Bizzeti , T. Blake⁵⁷ , F. Blanc⁵⁰ , J.E. Blank¹⁹ ,
S. Blusk⁶⁹ , V. Bocharnikov⁴⁴ , J.A. Boelhaue¹⁹ , O. Boente Garcia¹⁵ ,
T. Boettcher⁶⁶ , A. Bohare⁵⁹ , A. Boldyrev⁴⁴ , C.S. Bolognani⁸⁰ , R. Bolzonella^{26,l} , R.
B. Bonacci¹ , N. Bondar⁴⁴ , A. Bordelius⁴⁹ , F. Borgato³³ , S. Borghi⁶³ ,
M. Borsato^{31,o} , J.T. Borsuk⁴¹ , E. Botalico⁶¹ , S.A. Bouchiba⁵⁰ , M. Bovill⁶⁴ ,
T.J.V. Bowcock⁶¹ , A. Boyer⁴⁹ , C. Bozzi²⁶ , J. D. Brandenburg⁸⁶ ,
A. Brea Rodriguez⁵⁰ , N. Breer¹⁹ , J. Brodzicka⁴¹ , A. Brossa Gonzalo^{47,†} ,
J. Brown⁶¹ , D. Brundu³² , E. Buchanan⁵⁹ , L. Buonincontri^{33,p} , M.
Burgos Marcos⁸⁰ , A.T. Burke⁶³ , C. Burr⁴⁹ , J.S. Butter⁵⁶ , J. Buytaert⁴⁹ ,
W. Byczynski⁴⁹ , S. Cadeddu³² , H. Cai⁷⁴ , A. Caillet¹⁶ , R. Calabrese^{26,l} ,
S. Calderon Ramirez⁹ , L. Calefice⁴⁶ , S. Cali²⁸ , M. Calvi^{31,o} , M. Calvo Gomez⁴⁵ ,
P. Camargo Magalhaes^{2,z} , J. I. Cambon Bouzas⁴⁷ , P. Campana²⁸ ,
D.H. Campora Perez⁸⁰ , A.F. Campoverde Quezada⁷ , S. Capelli³¹ , L. Capriotti²⁶ ,
R. Caravaca-Mora⁹ , A. Carbone^{25,j} , L. Carcedo Salgado⁴⁷ , R. Cardinale^{29,m} ,
A. Cardini³² , P. Carniti^{31,o} , L. Carus²² , A. Casais Vidal⁶⁵ , R. Caspary²² ,
G. Casse⁶¹ , M. Cattaneo⁴⁹ , G. Cavallero^{26,49} , V. Cavallini^{26,l} , S. Celani²² , S.
Cesare^{30,n} , A.J. Chadwick⁶¹ , I. Chahrour⁸⁵ , H. Chang^{4,b} , M. Charles¹⁶ ,
Ph. Charpentier⁴⁹ , E. Chatzianagnostou³⁸ , M. Chefdeville¹⁰ , C. Chen¹³ , S. Chen⁵ ,
Z. Chen⁷ , A. Chernov⁴¹ , S. Chernyshenko⁵³ , X. Chiotopoulos⁸⁰ , V. Chobanova⁸² ,
M. Chrzaszcz⁴¹ , A. Chubykin⁴⁴ , V. Chulikov^{28,36} , P. Ciambone²⁸ , X. Cid Vidal⁴⁷ ,
G. Ciezarek⁴⁹ , P. Cifra⁴⁹ , P.E.L. Clarke⁵⁹ , M. Clemencic⁴⁹ , H.V. Cliff⁵⁶ ,
J. Closier⁴⁹ , C. Cocha Toapaxi²² , V. Coco⁴⁹ , J. Cogan¹³ , E. Cogneras¹¹ ,
L. Cojocariu⁴³ , S. Collaviti⁵⁰ , P. Collins⁴⁹ , T. Colombo⁴⁹ , M. Colonna¹⁹ ,
A. Comerma-Montells⁴⁶ , L. Congedo²⁴ , A. Contu³² , N. Cooke⁶⁰ , I. Corredoira⁴⁷ ,
A. Correia¹⁶ , G. Corti⁴⁹ , J. Cottee Meldrum⁵⁵ , B. Couturier⁴⁹ , D.C. Craik⁵¹ ,
M. Cruz Torres^{2,g} , E. Curras Rivera⁵⁰ , R. Currie⁵⁹ , C.L. Da Silva⁶⁸ , S. Dadabaev⁴⁴ ,
L. Dai⁷¹ , X. Dai⁴ , E. Dall'Occo⁴⁹ , J. Dalseno⁴⁷ , C. D'Ambrosio⁴⁹ , J. Daniel¹¹ ,
A. Danilina⁴⁴ , P. d'Argent²⁴ , G. Darze³ , A. Davidson⁵⁷ , J.E. Davies⁶³ ,
O. De Aguiar Francisco⁶³ , C. De Angelis^{32,k} , F. De Benedetti⁴⁹ , J. de Boer³⁸ ,

Y. Tan^{4,b} , Y. Tang⁷⁴ , M.D. Tat²² , A. Terentev⁴⁴ , F. Terzuoli^{35,v,49} , F. Teubert⁴⁹ , E. Thomas⁴⁹ , D.J.D. Thompson⁵⁴ , H. Tilquin⁶² , V. Tisserand¹¹ , S. T'Jampens¹⁰ , M. Tobin^{5,49} , L. Tomassetti^{26,l} , G. Tonani^{30,n} , X. Tong⁶ , T. Tork³⁰ , D. Torres Machado² , L. Toscano¹⁹ , D.Y. Tou^{4,b} , C. Trippi⁴⁵ , G. Tuci²² , N. Tuning³⁸ , L.H. Uecker²² , A. Ukleja⁴⁰ , D.J. Unverzagt²² , B. Urbach⁵⁹ , A. Usachov³⁹ , A. Ustyuzhanin⁴⁴ , U. Uwer²² , V. Vagnoni²⁵ , V. Valcarce Cadenas⁴⁷ , G. Valenti²⁵ , N. Valls Canudas⁴⁹ , J. van Eldik⁴⁹ , H. Van Hecke⁶⁸ , E. van Herwijnen⁶² , C.B. Van Hulse^{47,y} , R. Van Laak⁵⁰ , M. van Veghel³⁸ , G. Vasquez⁵¹ , R. Vazquez Gomez⁴⁶ , P. Vazquez Regueiro⁴⁷ , C. Vázquez Sierra⁴⁷ , S. Vecchi²⁶ , J.J. Velthuis⁵⁵ , M. Veltri^{27,w} , A. Venkateswaran⁵⁰ , M. Verdognia³² , M. Vesterinen⁵⁷ , D. Vico Benet⁶⁴ , P. Vidrier Villalba⁴⁶ , M. Vieites Diaz⁴⁷ , X. Vilasis-Cardona⁴⁵ , E. Vilella Figueras⁶¹ , A. Villa²⁵ , P. Vincent¹⁶ , F.C. Volle⁵⁴ , D. vom Bruch¹³ , N. Voropaev⁴⁴ , K. Vos⁸⁰ , C. Vrahas⁵⁹ , J. Wagner¹⁹ , J. Walsh³⁵ , E.J. Walton^{1,57} , G. Wan⁶ , C. Wang²² , G. Wang⁸ , H. Wang⁷³ , J. Wang⁶ , J. Wang⁵ , J. Wang^{4,b} , J. Wang⁷⁴ , M. Wang⁴⁹ , N. W. Wang⁷ , R. Wang⁵⁵ , X. Wang⁸ , X. Wang⁷² , X. W. Wang⁶² , Y. Wang⁶ , Y. W. Wang⁷³ , Z. Wang¹⁴ , Z. Wang^{4,b} , Z. Wang³⁰ , J.A. Ward^{57,1} , M. Waterlaan⁴⁹ , N.K. Watson⁵⁴ , D. Websdale⁶² , Y. Wei⁶ , J. Wendel⁸² , B.D.C. Westhenry⁵⁵ , C. White⁵⁶ , M. Whitehead⁶⁰ , E. Whiter⁵⁴ , A.R. Wiederhold⁶³ , D. Wiedner¹⁹ , G. Wilkinson⁶⁴ , M.K. Wilkinson⁶⁶ , M. Williams⁶⁵ , M. J. Williams⁴⁹ , M.R.J. Williams⁵⁹ , R. Williams⁵⁶ , Z. Williams⁵⁵ , F.F. Wilson⁵⁸ , M. Winn¹² , W. Wislicki⁴² , M. Witek⁴¹ , L. Witola²² , G. Wormser¹⁴ , S.A. Wotton⁵⁶ , H. Wu⁶⁹ , J. Wu⁸ , X. Wu⁷⁴ , Y. Wu⁶ , Z. Wu⁷ , K. Wyllie⁴⁹ , S. Xian⁷² , Z. Xiang⁵ , Y. Xie⁸ , T. X. Xing³⁰ , A. Xu³⁵ , L. Xu^{4,b} , L. Xu^{4,b} , M. Xu⁵⁷ , Z. Xu⁴⁹ , Z. Xu⁷ , Z. Xu⁵ , K. Yang⁶² , S. Yang⁷ , X. Yang⁶ , Y. Yang^{29,m} , Z. Yang⁶ , V. Yeroshenko¹⁴ , H. Yeung⁶³ , H. Yin⁸ , X. Yin⁷ , C. Y. Yu⁶ , J. Yu⁷¹ , X. Yuan⁵ , Y. Yuan^{5,7} , E. Zaffaroni⁵⁰ , M. Zavertyaev²¹ , M. Zdybal⁴¹ , F. Zenesini²⁵ , C. Zeng^{5,7} , M. Zeng^{4,b} , C. Zhang⁶ , D. Zhang⁸ , J. Zhang⁷ , L. Zhang^{4,b} , S. Zhang⁷¹ , S. Zhang⁶⁴ , Y. Zhang⁶ , Y. Z. Zhang^{4,b} , Z. Zhang^{4,b} , Y. Zhao²² , A. Zhelezov²² , S. Z. Zheng⁶ , X. Z. Zheng^{4,b} , Y. Zheng⁷ , T. Zhou⁶ , X. Zhou⁸ , Y. Zhou⁷ , V. Zhovkovska⁵⁷ , L. Z. Zhu⁷ , X. Zhu^{4,b} , X. Zhu⁸ , V. Zhukov¹⁷ , J. Zhuo⁴⁸ , Q. Zou^{5,7} , D. Zuliani^{33,p} , G. Zunica⁵⁰ .

¹*School of Physics and Astronomy, Monash University, Melbourne, Australia*

²*Centro Brasileiro de Pesquisas Físicas (CBPF), Rio de Janeiro, Brazil*

³*Universidade Federal do Rio de Janeiro (UFRJ), Rio de Janeiro, Brazil*

⁴*Department of Engineering Physics, Tsinghua University, Beijing, China*

⁵*Institute Of High Energy Physics (IHEP), Beijing, China*

⁶*School of Physics State Key Laboratory of Nuclear Physics and Technology, Peking University, Beijing, China*

⁷*University of Chinese Academy of Sciences, Beijing, China*

⁸*Institute of Particle Physics, Central China Normal University, Wuhan, Hubei, China*

⁹*Consejo Nacional de Rectores (CONARE), San Jose, Costa Rica*

¹⁰*Université Savoie Mont Blanc, CNRS, IN2P3-LAPP, Annecy, France*

¹¹*Université Clermont Auvergne, CNRS/IN2P3, LPC, Clermont-Ferrand, France*

¹²*Université Paris-Saclay, Centre d'Etudes de Saclay (CEA), IRFU, Saclay, France, Gif-Sur-Yvette, France*

¹³*Aix Marseille Univ, CNRS/IN2P3, CPPM, Marseille, France*

¹⁴*Université Paris-Saclay, CNRS/IN2P3, IJCLab, Orsay, France*

¹⁵*Laboratoire Leprince-Ringuet, CNRS/IN2P3, Ecole Polytechnique, Institut Polytechnique de Paris, Palaiseau, France*

¹⁶*LPNHE, Sorbonne Université, Paris Diderot Sorbonne Paris Cité, CNRS/IN2P3, Paris, France*

¹⁷*I. Physikalisches Institut, RWTH Aachen University, Aachen, Germany*

- ¹⁸ *Universität Bonn - Helmholtz-Institut für Strahlen und Kernphysik, Bonn, Germany*
- ¹⁹ *Fakultät Physik, Technische Universität Dortmund, Dortmund, Germany*
- ²⁰ *Physikalisches Institut, Albert-Ludwigs-Universität Freiburg, Freiburg, Germany*
- ²¹ *Max-Planck-Institut für Kernphysik (MPIK), Heidelberg, Germany*
- ²² *Physikalisches Institut, Ruprecht-Karls-Universität Heidelberg, Heidelberg, Germany*
- ²³ *School of Physics, University College Dublin, Dublin, Ireland*
- ²⁴ *INFN Sezione di Bari, Bari, Italy*
- ²⁵ *INFN Sezione di Bologna, Bologna, Italy*
- ²⁶ *INFN Sezione di Ferrara, Ferrara, Italy*
- ²⁷ *INFN Sezione di Firenze, Firenze, Italy*
- ²⁸ *INFN Laboratori Nazionali di Frascati, Frascati, Italy*
- ²⁹ *INFN Sezione di Genova, Genova, Italy*
- ³⁰ *INFN Sezione di Milano, Milano, Italy*
- ³¹ *INFN Sezione di Milano-Bicocca, Milano, Italy*
- ³² *INFN Sezione di Cagliari, Monserrato, Italy*
- ³³ *INFN Sezione di Padova, Padova, Italy*
- ³⁴ *INFN Sezione di Perugia, Perugia, Italy*
- ³⁵ *INFN Sezione di Pisa, Pisa, Italy*
- ³⁶ *INFN Sezione di Roma La Sapienza, Roma, Italy*
- ³⁷ *INFN Sezione di Roma Tor Vergata, Roma, Italy*
- ³⁸ *Nikhef National Institute for Subatomic Physics, Amsterdam, Netherlands*
- ³⁹ *Nikhef National Institute for Subatomic Physics and VU University Amsterdam, Amsterdam, Netherlands*
- ⁴⁰ *AGH - University of Krakow, Faculty of Physics and Applied Computer Science, Kraków, Poland*
- ⁴¹ *Henryk Niewodniczanski Institute of Nuclear Physics Polish Academy of Sciences, Kraków, Poland*
- ⁴² *National Center for Nuclear Research (NCBJ), Warsaw, Poland*
- ⁴³ *Horia Hulubei National Institute of Physics and Nuclear Engineering, Bucharest-Magurele, Romania*
- ⁴⁴ *Authors affiliated with an institute formerly covered by a cooperation agreement with CERN.*
- ⁴⁵ *DS4DS, La Salle, Universitat Ramon Llull, Barcelona, Spain*
- ⁴⁶ *ICCUB, Universitat de Barcelona, Barcelona, Spain*
- ⁴⁷ *Instituto Galego de Física de Altas Enerxías (IGFAE), Universidade de Santiago de Compostela, Santiago de Compostela, Spain*
- ⁴⁸ *Instituto de Física Corpuscular, Centro Mixto Universidad de Valencia - CSIC, Valencia, Spain*
- ⁴⁹ *European Organization for Nuclear Research (CERN), Geneva, Switzerland*
- ⁵⁰ *Institute of Physics, Ecole Polytechnique Fédérale de Lausanne (EPFL), Lausanne, Switzerland*
- ⁵¹ *Physik-Institut, Universität Zürich, Zürich, Switzerland*
- ⁵² *NSC Kharkiv Institute of Physics and Technology (NSC KIPT), Kharkiv, Ukraine*
- ⁵³ *Institute for Nuclear Research of the National Academy of Sciences (KINR), Kyiv, Ukraine*
- ⁵⁴ *School of Physics and Astronomy, University of Birmingham, Birmingham, United Kingdom*
- ⁵⁵ *H.H. Wills Physics Laboratory, University of Bristol, Bristol, United Kingdom*
- ⁵⁶ *Cavendish Laboratory, University of Cambridge, Cambridge, United Kingdom*
- ⁵⁷ *Department of Physics, University of Warwick, Coventry, United Kingdom*
- ⁵⁸ *STFC Rutherford Appleton Laboratory, Didcot, United Kingdom*
- ⁵⁹ *School of Physics and Astronomy, University of Edinburgh, Edinburgh, United Kingdom*
- ⁶⁰ *School of Physics and Astronomy, University of Glasgow, Glasgow, United Kingdom*
- ⁶¹ *Oliver Lodge Laboratory, University of Liverpool, Liverpool, United Kingdom*
- ⁶² *Imperial College London, London, United Kingdom*
- ⁶³ *Department of Physics and Astronomy, University of Manchester, Manchester, United Kingdom*
- ⁶⁴ *Department of Physics, University of Oxford, Oxford, United Kingdom*
- ⁶⁵ *Massachusetts Institute of Technology, Cambridge, MA, United States*
- ⁶⁶ *University of Cincinnati, Cincinnati, OH, United States*
- ⁶⁷ *University of Maryland, College Park, MD, United States*
- ⁶⁸ *Los Alamos National Laboratory (LANL), Los Alamos, NM, United States*
- ⁶⁹ *Syracuse University, Syracuse, NY, United States*
- ⁷⁰ *Pontifícia Universidade Católica do Rio de Janeiro (PUC-Rio), Rio de Janeiro, Brazil, associated to ³*
- ⁷¹ *School of Physics and Electronics, Hunan University, Changsha City, China, associated to ⁸*

⁷²Guangdong Provincial Key Laboratory of Nuclear Science, Guangdong-Hong Kong Joint Laboratory of Quantum Matter, Institute of Quantum Matter, South China Normal University, Guangzhou, China, associated to ⁴

⁷³Lanzhou University, Lanzhou, China, associated to ⁵

⁷⁴School of Physics and Technology, Wuhan University, Wuhan, China, associated to ⁴

⁷⁵Departamento de Física, Universidad Nacional de Colombia, Bogota, Colombia, associated to ¹⁶

⁷⁶Ruhr Universitaet Bochum, Fakultaet f. Physik und Astronomie, Bochum, Germany, associated to ¹⁹

⁷⁷Eotvos Lorand University, Budapest, Hungary, associated to ⁴⁹

⁷⁸Vilnius University, Vilnius, Lithuania, associated to ²⁰

⁷⁹Van Swinderen Institute, University of Groningen, Groningen, Netherlands, associated to ³⁸

⁸⁰Universiteit Maastricht, Maastricht, Netherlands, associated to ³⁸

⁸¹Tadeusz Kosciuszko Cracow University of Technology, Cracow, Poland, associated to ⁴¹

⁸²Universidad de Coruña, A Coruña, Spain, associated to ⁴⁵

⁸³Department of Physics and Astronomy, Uppsala University, Uppsala, Sweden, associated to ⁶⁰

⁸⁴Taras Schevchenko University of Kyiv, Faculty of Physics, Kyiv, Ukraine, associated to ¹⁴

⁸⁵University of Michigan, Ann Arbor, MI, United States, associated to ⁶⁹

⁸⁶Ohio State University, Columbus, United States, associated to ⁶⁸

^aCentro Federal de Educação Tecnológica Celso Suckow da Fonseca, Rio De Janeiro, Brazil

^bCenter for High Energy Physics, Tsinghua University, Beijing, China

^cHangzhou Institute for Advanced Study, UCAS, Hangzhou, China

^dSchool of Physics and Electronics, Henan University, Kaifeng, China

^eLIP6, Sorbonne Université, Paris, France

^fLamarr Institute for Machine Learning and Artificial Intelligence, Dortmund, Germany

^gUniversidad Nacional Autónoma de Honduras, Tegucigalpa, Honduras

^hUniversità di Bari, Bari, Italy

ⁱUniversità di Bergamo, Bergamo, Italy

^jUniversità di Bologna, Bologna, Italy

^kUniversità di Cagliari, Cagliari, Italy

^lUniversità di Ferrara, Ferrara, Italy

^mUniversità di Genova, Genova, Italy

ⁿUniversità degli Studi di Milano, Milano, Italy

^oUniversità degli Studi di Milano-Bicocca, Milano, Italy

^pUniversità di Padova, Padova, Italy

^qUniversità di Perugia, Perugia, Italy

^rScuola Normale Superiore, Pisa, Italy

^sUniversità di Pisa, Pisa, Italy

^tUniversità della Basilicata, Potenza, Italy

^uUniversità di Roma Tor Vergata, Roma, Italy

^vUniversità di Siena, Siena, Italy

^wUniversità di Urbino, Urbino, Italy

^xUniversidad de Ingeniería y Tecnología (UTEC), Lima, Peru

^yUniversidad de Alcalá, Alcalá de Henares, Spain

^zFacultad de Ciencias Físicas, Madrid, Spain

^{aa}Department of Physics/Division of Particle Physics, Lund, Sweden

† Deceased